

Design and Testing Radome for D-band applications

Arto Hujanen¹, Alexandros I. Dimitriadis², Jussi Säily¹, Vladimir Ermolov¹

¹ VTT Technical Research of Finland, Espoo 02044, Finland, vladimir.ermolov@vtt.fi

² SWISSto12 S.A., 1020 Renens, Switzerland, a.dimitriades@swisstol2.ch

Abstract—The paper presents results of characterization of dielectric properties of several commercial radome materials in D-band. It is demonstrated that there are commercial radome materials on the market already today which can be used for D-band radome. A multilayer radome based on selected materials Preperm RS260 and Rohacell HF is designed and tested. The radome demonstrates transmission losses not higher than 0.75 dB in the frequency band of 130 – 165 GHz. Usage of the radome in a combination with a D-band antenna array is studied.

Keywords— *D-band, radome, mmWave, dielectric constant, loss tangent.*

I. INTRODUCTION

DATA rates in wireless communications have been increasing exponentially over the recent decades. The requirement of a hundred Gbit/s demands the use of large bandwidths, which are available only in the high millimeter-wave and sub-terahertz regions [1, 2]. The D-band, ranging from 130 to 175 GHz, offers a vast bandwidth and is being considered as a candidate for a new approach to high capacity backhaul networks for 5G and beyond [3,4].

Radome is an important element of any communication or radar system. The radome is forming a barrier between an antenna and the environment and protecting the system against wind, rain, humidity, and other environmental influences allowing all weather operation of the system. The radome must have minimal impact on the electromagnetic performance of the antenna. The ideal radome would be electromagnetically transparent. Electromagnetic transparency means low reflection, low insertion loss, and minimum distortion of signal polarization. At the same time other requirements for the radome might include high impact strength, UV tolerance, low moisture absorption and a hydrophobic surface. The radome reduces the operation and maintenance cost of the system and increases its life span.

Different radome configurations are used, including half-wave, A-sandwich, double sandwiches, and multiple A-sandwiches [5]. The best-suited configuration for a particular application depends on the mechanical requirements of radome and its operating frequency. Based on the needs, radome can have different shapes such as planar, spherical, or even geodesic where the shape will have some influence on the radiation pattern for maximum achievable distance. Currently, many materials for radomes are available on the

market. However, there is very limited information about their applicability for usage at the D-band frequency range.

The paper presents results of characterization of several commercial radome materials in D-band; results of design and testing a multilayer D-band radome realized based on the selected radome materials. Usage of the radome in a combination with D-band antenna array is studied.

II. IMPACT OF RADOME MATERIAL PROPERTIES ON RADOME PERFORMANCE

Let's demonstrate requirements for radome materials of a half-wave radome, for example. The radome losses depend on the complex relative permittivity of the dielectric material and the operational frequency. The relative permittivity is given as

$$\epsilon_r = \epsilon_r' - j\epsilon_r'' \quad (1)$$

where ϵ_r' is the real part, also known as the (relative) dielectric constant, and ϵ_r'' is the imaginary part.

The radome material parameters are typically given as the real part ϵ_r' and the loss tangent defined as

$$\tan\delta = \epsilon_r'' / \epsilon_r' \quad (2)$$

The transmission (T) and reflection (R) coefficients of a single layer radome for normal incidence can be calculated as

$$\begin{aligned} T &= \frac{(1-\rho^2)e^{-jkd}}{1-\rho^2e^{-2jkd}}, \\ R &= \frac{\rho(1-e^{-2jkd})}{1-\rho^2e^{-2jkd}} \end{aligned} \quad (3)$$

where $\rho = \frac{1-\sqrt{\epsilon_r}}{1+\sqrt{\epsilon_r}}$, $k = \frac{2\pi\sqrt{\epsilon_r}}{\lambda_0}$, d is the radome thickness and λ_0 is the wavelength in air.

The thickness of the radome is selected as

$$d = \frac{n\lambda_0}{2\sqrt{\epsilon_r}} = \frac{n}{2}\lambda_{radome} \quad (4)$$

where $n=1,2,3, \dots$ and λ_{radome} is the wavelength inside the radome material at the desired centre frequency of operation.

Effect of ϵ_r and $\tan\delta$ on radome performance is shown in Figure 1.

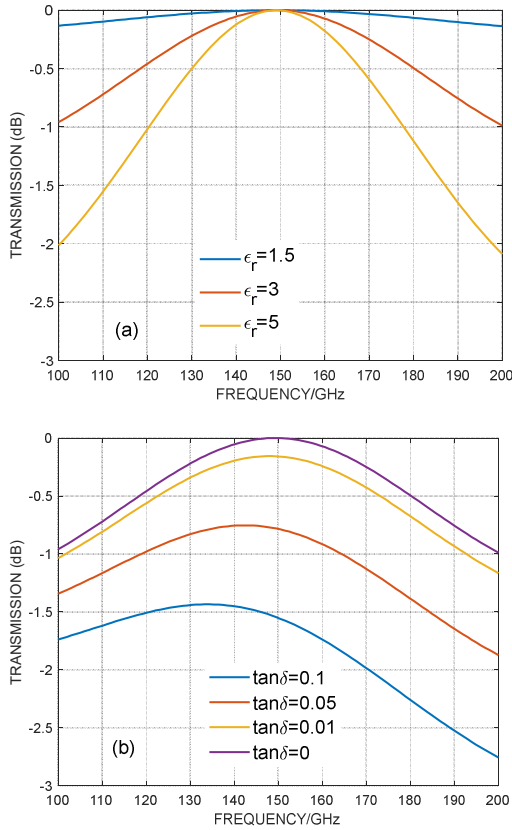


Figure 1. Transmission loss of a half-wave radome for (a) different dielectric constant and $\tan\delta=0$; (b) different dielectric constant and $\epsilon_r=3$.

Low dielectric constant allows to obtain higher operational bandwidth of the radome. A radome with correctly chosen thickness and $\tan\delta < 0.01$ results in a transmission loss that is only a fraction of a dB at the desired frequency. Thus, materials with lower dielectric constant and loss tangent are recommended for radome designs.

Usually, materials are used in radome having permittivity ranging from 1 to 5 and loss tangent from 0.001 to 0.01 [5]. The same values could be a good target for materials to be used in D-band radomes.

III. CHARACTERIZATION OF RADOME MATERIALS IN D-BAND

Review of radome materials promising for usage in D-band and present on market was done. The materials listed in Table 1 are selected for testing. There are commonly available materials, but also some special materials from specific companies. The system used for the D-band measurements is based on the Material Characterization Kit (MCK) fixture developed and commercialized by SWISSto12 S.A. [6]. The device is composed of two corrugated horn antennas with standard waveguide input ports, as shown in Figure 2. The

corrugated horns are used for producing a wideband symmetrical, gaussian beam that guarantee a beam waist almost like a plane wave in the material sample position.

Table 1. Samples for measurements

Sample	PTFE polytetrafluoroethylene	PE HD (Polyethylene high density)	PE 1000 (Polyethylene variant)				
Thickness / mm	5.70	5.05	5.05				
Sample	PP (Polypropylene)	PC (Polycarbonate)	Rexolite 1422				
Thickness / mm	4.90	4.80	4.95				
Sample	Preperm RS260 ¹	Rohacell HF	E1 ²				
Thickness / mm	0.80	2.00	2.90				
Sample	E2 ²	E3 ²	E4 ²	E5 ²	S1 ³	S2 ³	S3 ³
Thickness / mm	0.3	0.3	2.11	1.57	0.15	0.21	0.20

¹ Material sample from Vendor 1

² Material sample from Vendor 2

³ Material sample from Vendor 3

The first antenna (connected to VNA test port 1) is mechanically fixed and the second one (connected to VNA test port 2) is movable, so that the material under test (MUT) can be accommodated in the gap between their apertures. The operating principle of this device is similar to free-space measurement techniques but with the additional advantage of automatic sample alignment by construction.

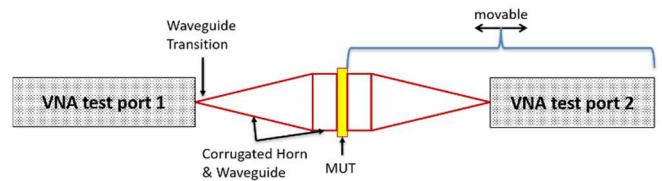


Figure 2. Schematic of the MCK test system.

In the measurement setup, the MCK has been connected to two VNA6.5 frequency extenders with standard waveguide output ports from Virginia Diodes [7]. The VNA used for the measurements was a 4-port Keysight PNA N5244A with time-gating option enabled.

For the measurements, a simple two-step calibration procedure has been used to normalize the reflection (S_{11}) and transmission (S_{21}) measurements [8]. A dedicated software enables automatic data acquisition from the VNA to an external computer for further post-processing. Permittivity and loss tangent values are then obtained by a simple least-square minimization routine that is based on the analytical formulas presented in Eq. (3).

The accuracy of this measurement technique depends mainly on the quality of the samples, most notably the planarity of their faces. Provided that the sample preparation ensures a good planarity and surface roughness of the parts, permittivity values are measured with approximately 2% accuracy, while loss tangent exhibits a typical accuracy of 10%. This value is lower for samples with higher losses (since the uncertainty of the S_{21} measurement is lower) than for low loss samples; typically, measurements of samples with a loss tangent below $5e-3$ are not very reliable and repeatable and a resonant method is recommended instead.

Measurement results and fitted theoretical plots for a sample with homogenous structure (Preperm RS260) and a sample with fabric structure (E1) are presented in Figure 3 and 4 as examples. It was found that it is possible to reach good fitting for the homogeneous samples (see Figure 3).

However, for samples with fabric structures the measured and modelled curves are not fitted very well (see Figure 4). The same behaviour is observed for other samples.

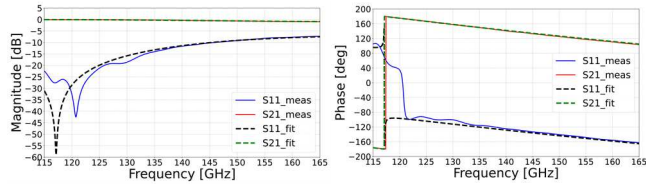


Figure 3. Measured S parameters and fitted theoretical lines for Preperm RS260 sample with a thickness of 0.80 mm. The best fit is observed for the values $\epsilon_{ps}' = 2.559$ and $\tan\delta = 1.452e-3$.

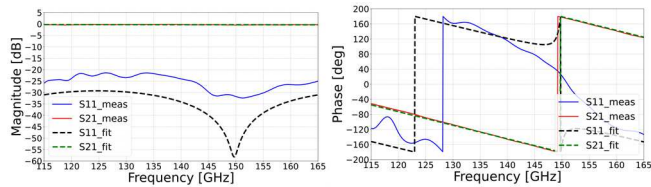


Figure 4. Measured S parameters and fitted theoretical lines for E1 sample with a thickness of 2.90 mm. The best fit is observed for the values $\epsilon_{ps}' = 1.073$ and $\tan\delta = 7.618e-3$.

The results are as expected because the waveguide method is developed for testing homogeneous materials. As it was pointed above, the accuracy of measurement by the waveguide method at D-band is few percent for the dielectric constant (ϵ_r) and tens of percent for loss factor ($\tan\delta$). However, the error can be even higher for the case of inhomogeneous fabric materials. The main reason for that is the measurement uncertainty for transmission when a very thin, low-loss sample is introduced in the test setup. Especially with such high-frequency setups using frequency extenders, the amplitude and phase stability for S21 measurements impose certain limitations to the precision of the MCK measurements.

However, results of testing are allowing to make general conclusions about the applicability of materials in D-band radomes, even in the cases of fabric materials. Summary of the test results for all selected materials is presented in Table 2

Table 2. Summary of the measured properties of the tested materials.

	Samples (1/2)							
	<i>PTFE</i>	<i>PE HD</i>	<i>PE 1000</i>	<i>PP</i>	<i>PC</i>	<i>Rexo-litel</i>	<i>Pre-perm</i>	<i>E1</i>
thick-ness	5.70	5.05	5.05	4.90	4.80	4.95	0.80	2.90
ϵ_{ps}'	2.052	2.277	2.237	2.250	2.725	2.465	2.559	1.073
$\tan\delta$ ($1e-3$)	2.695	1.941	1.944	2.096	10.34	2.781	1.452	7.618

	Samples (2/2)							
	<i>Roha-cell</i>	<i>E2</i>	<i>E3</i>	<i>E4</i>	<i>E5</i>	<i>S1</i>	<i>S2</i>	<i>S3</i>
thick-ness	2.00	0.30	0.30	2.11	1.57	0.15	0.21	0.2
ϵ_{ps}'	1.030	3.304	3.595	2.844	4.479	2.400	2.465	1.517
$\tan\delta$ ($1e-3$)	7.589	32.15	36.52	61.81	29.90	32.26	10.66	97.62

The results presented above demonstrate that there are several commercial radome materials on market already today which can be used in D-band radomes.

IV. DESIGN AND TESTING OF THE MULTI LAYER RADOME

In this section we demonstrate design and testing of a multi-layer radome for D-band based on two materials: Preperm RS260 and Rohacell HF foam. A triple layer radome structure with Preperm RS260 as outer layers and Rohacell HF foam as an inner layer is selected. However, in practice, the layers of the radome must be glued together. We use Nitto 597B double-coated adhesive tape for gluing. These two extra gluing layers are also included in the simulated model. They are only 70 μm thick, which is very important because they are the lossiest material used in the structure ($\epsilon_{ps}' = 2.07$ and $\tan\delta = 60e-3$). Dielectric properties of Nitto tape are measured at 10-50 GHz frequency range by a resonance method and extrapolated for 150 GHz. Simulations are done with Matlab code based on a transmission line method. Figure 6 shows the simulated transmission of three-layer radome with two adhesive tape layers. Layer thicknesses are 0.57 mm for Preperm RS260, 0.5 mm for Rohacell HF and 70 μm for Nitto 597B tape. Free space measurement is used for testing the radome. Figure 5 shows the measurement setup.

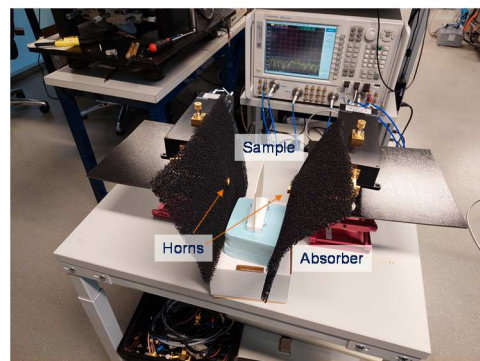


Figure 5. Measurement setup for radome testing.

The setup is built around two D-band horn antennas. Comparison of transmission measurements without and with the radome are done. Measurements are done in the frequency range of 110-170 GHz. An VNA Agilent N5245A - PNA-X and frequency extender modules VDI VNAX-WR6.5 were used for the measurements. Known standard gain horns were connected to extender ports. The measurement horn antennas are covered by absorbing material for avoiding multiple reflections between horns (Figure 5).

It is found that there are some reflections from environment even with usage of the absorbing material. To extract unwanted reflected signals, the measured signal is transformed into the time domain. Then the signal is gated, and the gated signal is transformed back to the frequency domain. The accuracy of radome transmission measurement is estimated to be about ± 0.25 dB.

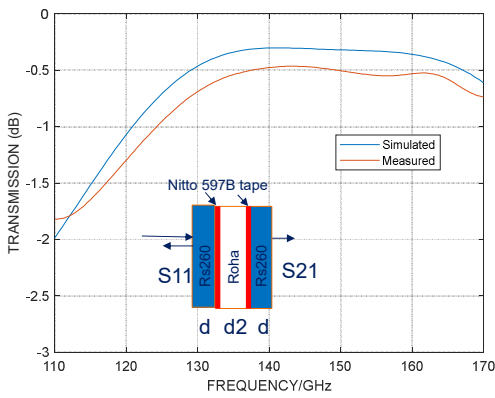


Figure 6. Transmission properties of the multi-layer radome with adhesive tape simulated and measured.

Results of radome testing are presented in Figure 6. The measured transmission is very similar to the simulated if the measurement accuracy (± 0.25 dB) is taken into account.

V. UTILIZATION OF THE RADOME WITH AN ANTENNA ARRAY

It was demonstrated that for real applications the number of elements in a D-band antenna array should be at least 1000 to provide the needed gross system gain [4].

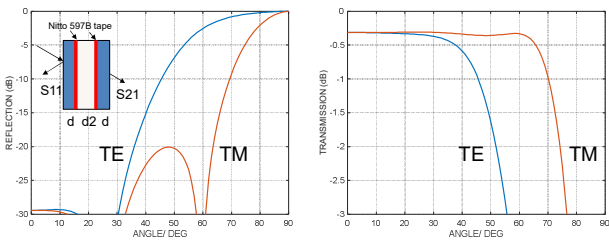


Figure 7 Simulated angle dependence of reflection and transmission properties of a triple layer radome with adhesive tape (TE- and TM-polarizations, $f=150$ GHz).

In such case, the size of the radome is considerably higher than the size of an antenna element and it could have an impact on the antenna performance. In this work we study specific usage of the radome with an antenna array in D-band. Figure 7 presents the incident angle dependence of reflection and transmission for TE and TM polarizations. The radome works well when incident angle is smaller than 40° for TE-polarization and smaller than 65° for TM polarization. If incident angles are more than these values, a considerable part of antenna emission will be reflected. These reflections could influence the impedance of antenna array elements.

The effect could be especially strong, if the distance between the radome and antenna elements is small. The effect is demonstrated in Figure 8. Let's make a simple estimation of the effect. A model includes two identical array elements placed at a distance R_{ele} as it is shown in Figure 8b.

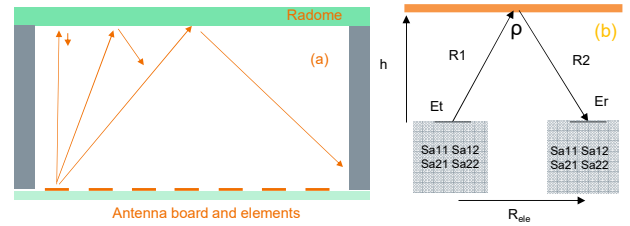


Figure 8. (a) Reflection between antenna elements caused by the radome, (b) simple mutual coupling model between antenna array elements.

The radome is placed at a distance h above the elements. Let's assume for simplicity also that $Sa_{12}=S_{21}=1$ and $Sa_{22}=0$. The S_{11} of each element can then expressed in form

$$S_{11} = \frac{a^-}{a^+} = Sa_{11} + \sqrt{1 - Sa_{11}^2} \rho \lambda \frac{e^{-jk2h}}{4\pi 2h} \quad (5)$$

where Sa_{11} is the antenna S_{11} without radome, ρ is the reflection coefficient of the radome, λ is wavelength, $k=2\pi/\lambda$ and h is the distance between radome and antenna array.

When all the elements are excited in the array the antenna element matching is changed due the mutual coupling. The active impedance (or active S_{11}) can be expressed in form

$$Sact_{11} \approx Sa_{11} + 2 \sum_{n=0}^N \sum_{m=0}^M \sqrt{1 - S_{11}^2} \rho \lambda \frac{e^{-jkR}}{4\pi R} \quad (6)$$

where

$R = R1 + R2 = 2 * \sqrt{\left(\frac{nd_x}{2}\right)^2 + \left(\frac{nd_y}{2}\right)^2 + h^2}$ and d_x, d_y is the element separation in wavelengths in a plane of the antenna array.

Figure 9 shows how the radome will change the impedance of a center antenna element in a 32×32 rectangular antenna

array for different radome distances. Simulations are done with Matlab code based on (5) and (6). The figure shows S_{11} and $S_{act_{11}}$, which demonstrate antenna impedance when the element is radiating, and other elements of the array are terminated or exited respectively. Element distance is 0.5λ in both x - and y - directions. Antenna impedance matching is supposed to be -20 dB. Simulations are done for values of reflections from radome at -10 dB or -20 dB. The reflection from radome may disturb the antenna matching if the radome reflection is high or if the radome is very near the antenna.

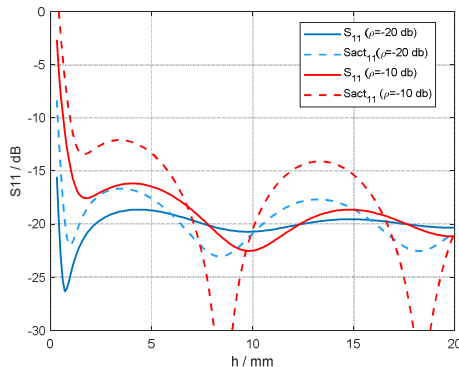


Figure 9. Effect of distance between the radome and an antenna array (h) on center element impedance of 32×32 rectangular antenna array element. Element distance is 0.5λ in element original $S_{11} = -20$ dB without radome, radome reflection coefficient of -20 dB and -10 dB.

However, even few millimetres separation between the array and the radome improves matching considerably. Figure demonstrates that low reflection from a radome is very important in broadband applications.

VI. CONCLUSIONS

Results of characterization of several commercial radome materials in D-band are presented. It is demonstrated that

there are several commercial radome materials on market already today which can be used in D-band radomes. A multi-layer radome based of selected materials is designed and tested. The multi-layer structure is selected because it is broadband and mechanically more robust. Observed radome transmission losses are about 0.5 dB at 150 GHz. Usage of radome in combination with an antenna array is studied for a realistic D-band application. It is demonstrated that the distance between radome and antenna elements should be a few millimeters or more for avoiding an effect of the radome on antenna element matching.

ACKNOWLEDGMENT

This work was conducted within the framework of the H2020 DRAGON project, which is partially funded by the Commission of the European Union (Grant Agreement No. 955699).

REFERENCES

- [1] M. Jaber, M. A. Imran, R. Tafazolli and A. Tukmanov, "5G Backhaul Challenges and Emerging Research Directions: A Survey," in *IEEE Access*, vol. 4, pp. 1743-1766, 2016.
- [2] Dimitris Siomos: ETSI ETSI GR mWT 012 V1.1.1: 5G Wireless Backhaul/X-Haul.
- [3] Y. Li and J. Hansryd, "Fixed Wireless Communication Links Beyond 100 GHz," 2018 Asia-Pacific Microwave Conference (APMC), Kyoto, Japan, 2018, pp. 31-33.
- [4] M. G. L. Frecassetti et al "D-Band Transport Solution to 5G and Beyond 5G Cellular Networks," European Conference on Networks and Communications (EuCNC), Valencia, Spain, Jun. 2019.
- [5] Z. Qamar, N. Aboserwal and J. L. Salazar-Cerreno, "An Accurate Method for Designing, Characterizing, and Testing a Multi-Layer Radome for mm-Wave Applications," in *IEEE Access*, vol. 8, pp. 23041-23053, 2020, doi: 10.1109/ACCESS.2020.2970544.
- [6] MCK Website: <https://mck.swissto12.ch/>.
- [7] VNA frequency extenders from Virginia Diodes: <https://www.vadiodes.com/en/products/vector-network-analyzer-extension-modules>.
- [8] Y. Wang et al., "Material Measurements Using VNA-Based Material Characterization Kits Subject to Thru-Reflect-Line Calibration," in *IEEE Transactions on Terahertz Science and Technology*, vol. 10, no. 5, pp. 466-473, Sept. 2020, doi: 10.1109/TTHZ.2020.2999631.